An optimized controller for ARGOS: using multiple wavefront sensor signals for homogeneous correction over the field

D. Peter[a]

[a]Max-Planck-Institut für Astronomie, Koenigstuhl 17, Heidelberg, Germany

ABSTRACT

ARGOS is the ground layer adaptive optics system planned for the LBT. The goal of such a ground layer adaptive optics system is to provide a maximum homogeneity of the point spread function over the full field of view. Controllers for optimized correction with an adaptive optics system with guide star and science target at different field angles are well known in the case of a single guide star. As ARGOS uses three laser guide stars and one auxiliary natural guide star a weighting scheme is required to optimize the homogeneity using all available information. Especially the tip and tilt modes measured by the one single off axis guide star and estimated thereof over the field will need to be improved by incorporation of the laser measurements. I will present the full scheme for an optimized controller for the ARGOS system. This controller uses the wavefront signals of the three lasers to additionally reconstruct the lower atmosphere. Information on the higher atmosphere will be provided by a DIMM-MASS instrument. The control scheme is tested analytically and the variation of the point spread function is then measured over the full field.

Keywords: Adaptive optics, ground layer AO, Controller, wide field

1. THE ARGOS SYSTEM

ARGOS[1] is the ground layer adaptive optics (GLAO) system for the LBT. The system recently passed the final design review and is planned to be at the telescope at mid 2012. It is designed to act as seeing reducer for the LUCIFER[2] instrument. The goal is to reduce the full width at half maximum (FWHM) on the science image by a factor of two for a wide range of atmospheric conditions. This will improve the spatial resolution on the image and save observing time. A schematic image of ARGOS is shown in Figure 1.

Further on ARGOS aims at providing a good homogeneity of the point spread function (PSF) over the full field of view (FOV). As ARGOS only uses one natural guide star to correct atmospheric TT-aberrations the major inhomogeneities over the FOV will be the result of TT-anisoplanatism. To compensate this anisoplanatism an optimal control scheme is derived which incorporates the high order (HO) laser measurements into the TT-estimation.

In the following I will describe the details of the system relevant for this paper. The discussion will take place on a single eye of the telescope as there is no interaction foreseen between the parts of the ARGOS system for each eye of the telescope.

For measurement of high order (HO-)modes ARGOS will use three green (532nm) Rayleigh-laser guide stars (LGS) which are positioned on a circle ' radius at a height of 12 km. The lasers will be equally spaced on the circle, i.e., with an angle of 120° between them. The measurement is done by three 15x15 Shack Hartmann sensors (SWS).

The Tip-Tilt (TT-)modes will be measured by a TT-wavefront sensor (WFS) using a natural guide star. This star can be anywhere in the field of view (FOV) of LUCIFER which is 4' x 4'. The measurement is done by a quad cell detector. Additionally there is an external DIMM-MASS[3,4] instrument to measure atmospheric seeing and provide a C_N^2 profile. From this data the wavefront is reconstructed, and the reconstructed wavefront is applied to the adaptive secondary mirror of the telescope.

Further author information: (Send correspondence to D.Peter)
D.Peter: E-mail: peterd@mpia.de, Telephone: 0049 6221 528394

Adaptive Optics Systems II, edited by Brent L. Ellerbroek, Michael Hart, Norbert Hubin, Peter L. Wizinowich,
Proc. of SPIE Vol. 7736, 773615 · © 2010 SPIE · CCC code: 0277-786X/10/$18 · doi: 10.1117/12.857012

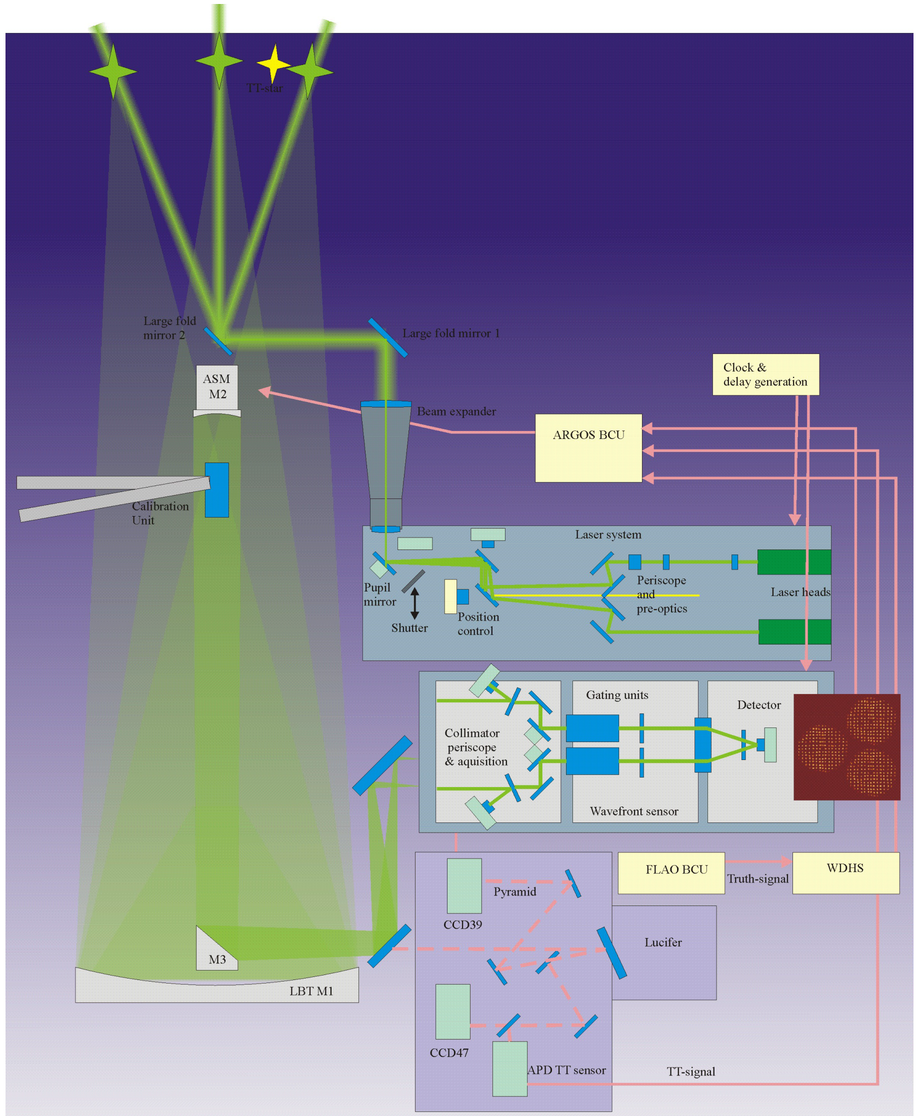

Figure 1. Sketch of the ARGOS system (courtesy of Sebastian Rabien)

1.1 Measurements and atmospheric parameters

To derive a scheme for an optimized controller it is important to know which data about the atmosphere is available. In the following the information which can be gathered will be outlined.
ARGOS provides five independent measurements to characterize the atmospheric disturbances on the incoming beam:

- three laser WFS
- one TT-WFS
- an external DIMM-MASS instrument.

These five sensors provide a wealth of information. The entire atmosphere, however, can only be measured by the TT-WFS and the DIMM-MASS instrument. From the TT-WFS the TT-mode of the atmosphere in the direction of the TT-star is measured and the DIMM-MASS instrument measures the seeing as well as a coarse atmospheric profile.

The three LGS-WFS measure the lower atmosphere only. Each of them can measure the wavefront error produced by the lower atmosphere in the direction of each LGS. Combining every two WFS-signals one can extract the C_N^2 profile of the lower atmosphere by a SLODAR[5] measurement. Via a (temporal) Periodogramm of the (spatial) power spectrum of the wavefront measured by the different LGS-WFS, the wind profile can be derived.[6] Table 1 outlines the different measurements, the parameters which can be extracted from them, and the method how this is done.

Table 1. Measured and calculated parameters of the atmosphere

	Measurement	Parameter	Method
single laser WFS*	slopes	HO-modes	AO reconstruction
two laser WFS*	slope spatial correlations	C_N^2 profile	SLODAR
two laser WFS*	slope spatio-temporal correlations	wind profile	SLODAR
TT WFS	slopes	TT-modes	AO reconstruction
DIMM-Mass	differential image motion	seeing,C_N^2 profile	DIMM-MASS

From this wealth of information only the pure spatial measurements will be used in the following. Never the less the wind profile is mentioned for completeness. It could be used for wavefront prediction. This prediction, however, is not subject of this paper.

The remaining paper is structured as follows: In the next Section the optimized control scheme is derived. In Section 3 the gain of the optimization over the non-optimized case is presented for a typical set-up. Section 4 concludes the paper.

2. THE OPTIMIZED CONTROL SCHEME

As a basis for the controller of the ARGOS system I use the MMSE control scheme derived by Whiteley et al.[7] They derive the minimum mean square error (MMSE) controller by the calculation of inter-aperture correlations of Zernike modes. The geometry underlying these calculations is shown in Figure 2. The wavefront in the direction of the science beam is calculated from the wave front measured in the direction of the laser. The angle between the two beams is 'A'. The optimized controller uses the inter-aperture correlations between the footprint of the laser beam on the atmospheric screen and the footprint of the science beam. As it will be needed later on I will shortly derive the expression for the MMSE controller for a single layered atmosphere.

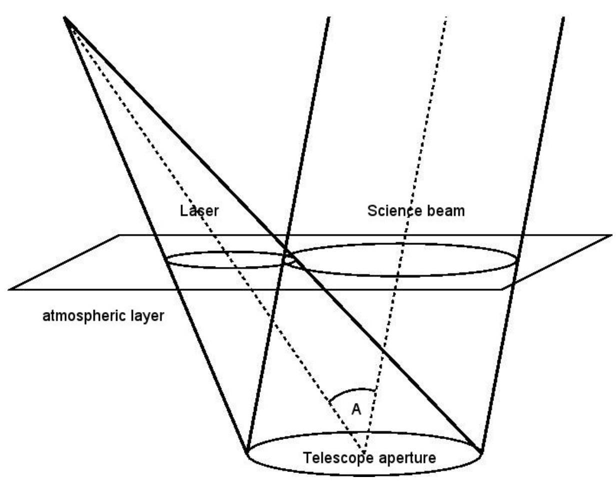

Figure 2. The geometry to derive the inter-aperture correlation matrices of the Zernike modes

The starting point is the total mean square error (MSE) of the wavefront, ϵ^2:

$$\epsilon^2 = \int d\rho W(\rho) < (\phi_0(R\rho) - \tilde{\phi}(R\rho))^2 > \quad (1)$$

where ϕ_0 the wavefront in the direction of the target, $\tilde{\phi}$ is the estimate of the wavefront, R the pupil radius, $<,>$ means ensemble average, and W the pupil function i.e.

$$W(\rho) = \begin{cases} \pi^{-1} & \text{if } \rho \leq 1 \\ 0 & \text{else} \end{cases} \tag{2}$$

The coefficient a_i of the 'i'th Zernike mode $Z_i(\rho)$ of any wavefront ϕ can be calculated as:

$$a_i = \int d\rho W(\rho) Z_i(\rho) \phi(R\rho) \tag{3}$$

applying Equation 3 to Equation 1 yields

$$\epsilon^2 = \int d\rho W(\rho) < (\phi_0(R\rho))^2 > + \sum_{i=2}^{N} [-2 < y_i, x_i > + < x_i, x_i >] \tag{4}$$

with y_i the coefficient of the wavefront in the direction of the target and x_i the coefficients of the estimate of this wavefront. Here all modes from Tip-tilt (i=2) up to mode number 'N' are reconstructed.
To arrive at the desired result the best estimate of the Zernike coefficients $\tilde{x_i}$ is expressed as the matrix product of a matrix P_{ij} and the Zernike coefficients x_j measured in guide star direction. In the following I will call P_{ij} the projector as it estimates the wavefront in one direction from the measurement of the wavefront in another direction. By optimizing the entries of P_{ij} the MSE is minimized:

$$\epsilon^2 = \int d\rho W(\rho) < (\phi_0(R\rho))^2 > + \sum_{i=2}^{N} \sum_{j=j_0}^{N_j} \left[-2P_{ij} < y_i, x_j > + \sum_{l=j_0}^{N_j} P_{ij} P_{il} < x_j, x_l > \right] = min \tag{5}$$

Here the wavefront is reconstructed from the modes 'j_0' up to 'N_j' measured on the wavefront sensor.
Taking the derivative of Equation 5 with respect to P_{kl} yields

$$- < y_l, x_m > + \sum_{j=j_0}^{N_j} P_{lj} < x_j, x_m >= 0 \tag{6}$$

which in matrix notation reads

$$- < y, x > + P < x, x >= 0. \tag{7}$$

Thus:

$$P =< y, x >< x, x >^{-1} \tag{8}$$

This is the MMSE controller of Whiteley et al.[7]
For the ARGOS system the derivation of the optimized controller must be extended for the case of multiple targets, as ARGOS is supposed to correct over the full FOV, and multiple sources, as ARGOS uses three laser guide stars and one TT-star, respectively.

2.1 Optimizing for multiple targets

Suppose one wants to observe more than one object or an extended object then the optimization should be applied in every direction of choice at the same time. The extreme case of this scheme will be the optimization over the entire FOV. The optimized controller for this application can be easily derived from an extension of equation 5:

$$\epsilon^2 = \int d\rho W(\rho) < (\phi_0(R\rho))^2 > + \sum_{i=2}^{N} \sum_{j=j_0}^{N_j} \left[-2 \sum_{t=1}^{N_{targets}} P_{ij} < y_i(t), x_j > + \sum_{l=j_0}^{N_j} P_{ij} P_{il} < x_j, x_l > \right] = min \tag{9}$$

Here the sum over 't' is the sum over different directions and $N_{targets}$ is the number of the targets for which the scheme is optimized. The solution of the optimization process is:

$$P = 1/N_{targets} \sum_{t=1}^{N_{targets}} < y(t), x >< x, x >^{-1} . \tag{10}$$

Thus, the final projector is just the average over the various projectors in every single direction.

2.2 Optimizing with multiple sources

An optimization for multiple sources is as straight forward as the optimization over multiple targets. Here I will show the example of two sources and one target as this is important for the later discussion of optimized TT-correction over the full field.
The term to optimize reads:

$$\epsilon^2 = \int d\rho W(\rho) < (\phi_0(R\rho))^2 > + \sum_{i=2}^{N} \left[-2 \sum_{j=j_0}^{N_j} P_{1ij} < y_i, x_{1j} > + \sum_{j,l=j_0}^{N_j} P_{1ij} P_{1il} < x_{1j}, x_{1l} > + \right. \tag{11}$$

$$\left. 2 \sum_{j=j_0}^{N_j} \sum_{k=k_0}^{N_k} P_{1ij} P_{2ik} < x_{1j}, x_{2k} > -2 \sum_{k=k_0}^{N_k} P_{2ik} < y_i, x_{2k} > + \sum_{k,m=k_0}^{N_k} P_{2ij} P_{2ik} < x_{2j}, x_{2k} > \right] = min$$

Taking the derivative wrt. P_{1kl} and P_{2kl} respectively results in the following equations:

$$- < y_l, x_{1m} > \quad + \quad \sum_{j=j_0}^{N_j} P_{1lj} < x_{1j}, x_{1m} > + \sum_{k=k_0}^{N_k} P_{2lk} < x_{2k}, x_{1m} > = 0$$

$$- < y_l, x_{2m} > \quad + \quad \sum_{k=k_0}^{N_k} P_{2lk} < x_{2k}, x_{2m} > + \sum_{j=j_0}^{N_j} P_{1lj} < x_{1j}, x_{2m} > = 0. \tag{12}$$

with the solutions:

$$P_1 = (< y, x_2 >< x_2, x_2 >^{-1} < x_2, x_1 > - < y, x_1 >)(< x_1, x_2 >< x_2, x_2 >^{-1} < x_2, x_1 > - < x_1, x_1 >)^{-1} \tag{13}$$

$$P_2 = (< y, x_1 >< x_1, x_1 >^{-1} < x_1, x_2 > - < y, x_2 >)(< x_2, x_1 >< x_1, x_1 >^{-1} < x_1, x_2 > - < x_2, x_2 >)^{-1} \tag{14}$$

Note that these expressions include that source 1 and source 2 are at different positions and different mode numbers are measured, e.g., x_1 is the mode vector of the TT-star, i.e., containing only the TT-modes, whereas x_2 is the mode vector of a laser guide star, i.e., containing purely HO-modes.

3. INCLUDING THE LASER MEASUREMENTS IN THE TT-CORRECTION

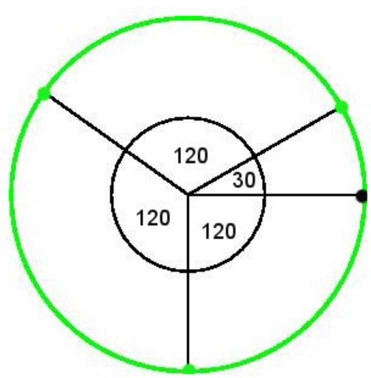

Figure 3. The geometry of the guide stars. The black dot marks the TT-star, the green dots mark the lasers. The numbers give the respective angles between the guide stars.

In the standard scheme for the optimized controller the modes in the direction of the target are estimated as linear combinations of the modes in the direction of the guide star, i.e., target TT-modes are constructed

from the TT-modes and the HO-modes of the same guide star. In the case of ARGOS the TT-modes and the HO-modes are measured at different field-angles. Thus the correlation between the off-axis modes and on-axis modes is different for TT-modes and HO-modes.
For the control scheme of ARGOS potentially three lasers can be included in the wave front measurement. As the control scheme is still under development, to get an estimate of the improvement of the correction over the field in this paper, I will not extend the control scheme (i.e. Equation 14) to optimize over all three laser measurements simultaneously. Rather, to estimate the benefit from including the laser WFS measurements in the control scheme, I will investigate the configurations for a fixed TT-star and each of the three lasers separately. The final MSE-map will then be a combination of the smallest contribution of the three parts. This method should give a good feeling how much the laser signals can be used to improved the performance.
In the calculations the atmosphere is modelled with six layers at 0 km, 3 km, 5 km, 7 km 10 km and 15 km height with an r_0 of 10 cm at 500nm and a relative C_N^2-profile of 0.4, 0.2, 0.1, 0.1, 0.1, 0.05. The outer scale was chosen to be 20m. The telescope diameter is 8.4m. The lasers are positioned at 12 km height at 2' from the field center with position angles of 30°, 150°, and 270° (see Figure/refimg:Guidestars). The TT star is at 2' from the field center at an position angle of 0°. For the optimized controller 33 modes (Zernike 4-36) were used from the laser measurement.
As I want to investigate the principle potential benefit of the optimization scheme no additional error terms are taken into account.
The observation is performed in K-band (at 2.2μm). As measure of the improvement in the performance the TT-MSE

$$\epsilon^2 = \sum_{i=2}^{3} < y_i, y_i > -2 < y_i, \tilde{x}_i > + < \tilde{x}_i, \tilde{x}_i > \tag{15}$$

of the optimized system is compared to the TT-MSE of the non-optimized system.
From the total wavefront MSE I will calculate the FWHM of the resulting PSF. This FWHM is closely related to the wavefront MSE as the peak to valley (PV) of the TT-modes is proportional to the root mean square (rms) MSE of the TT-wavefront. As a first attempt I will investigate the improvement in performance for the optimization in a single direction in Section 3.1. In Section 3.2 then the optimization is done for the full FOV and the improvement in wavefront MSE as well as the homogeneity over the full FOV are commented.

3.1 TT Optimization in a single direction

The first application of the control scheme is the optimization in a single direction. For the application as controller this scheme will be used more seldom than the optimization over a larger FOV. However, the scheme is very useful for an optimization of the PSF reconstruction[8] as there the best estimate of the wavefront in one specific direction is needed.
Figure 4 shows a comparison between the TT-MSE (Eq.15) over the FOV of a non-optimized system and the TT-MSE over the FOV of a system optimized in the specific field direction, i.e., any point on the plot shows the TT-MSE optimized for this position only. The FOV is 4' x 4', the resolution of the MSE map is 20".
To quantify the improvement resulting from the optimization of the controller the maximum TT-MSEs as well as the TT-MSE averaged over the FOV are calculated. For the case simulated above the ratio between maximum MSE of the optimized system, $\epsilon^2_{max-Opt}$, and the maximum MSE of the non-optimized system, ϵ^2_{max-NO}, is $\epsilon^2_{max-Opt}/\epsilon^2_{max-NO} = 0.64$. For the average values of the MSE, i.e., ϵ^2_{av} the ratio numbers:$\epsilon^2_{av-Opt}/\epsilon^2_{av-NO} = 0.73$. So the improvement is about 30%.

To better visualize the result the MSE is translated into a FWHM of the stellar images. Figure 5 shows the resulting PSF-map over the full FOV. The FOV is 4' x 4', the separation of the stars is 20" , and the pixel scale of the star field is 0."25. Only the TT-error was taken into account. The ratio between the maximum FWHM of the optimized system and the maximum FWHM of the non-optimized system is 0.8. For the average value of the FWHM this number is 0.85.

Figure 6 shows the MSE with distance from the TT-star. The solid line marks the result for the non-optimized system, the dashed line the result for the optimized system. At the furthest point the improvement is almost a factor of 2. The average value is marked by the asterisks on each curve.
At the furthest point the improvement of the TT-MSE is almost a factor of 2.

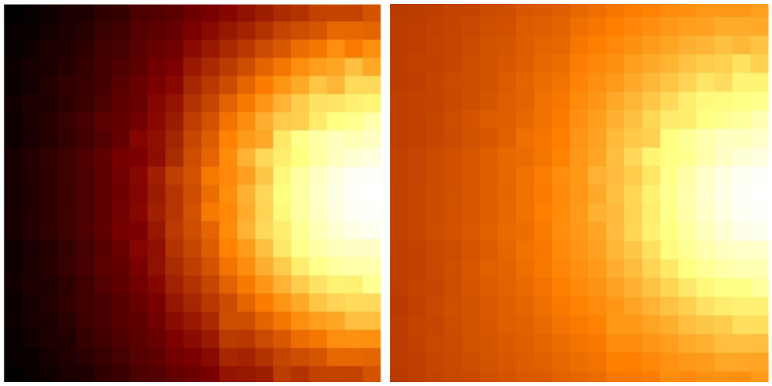

Figure 4. Comparison between the MSE of a system using purely the TT-modes for correction and a system including the optimized scheme. The FOV is 4' x 4', the resolution of the MSE map is 12". The color scale is the same for both maps. Left: TT-MSE correcting only the TT-modes, right: TT-MSE for the optimized system. Note that the map shows the minimum achievable MSE at every position, i.e., the controller is optimized for this direction only.

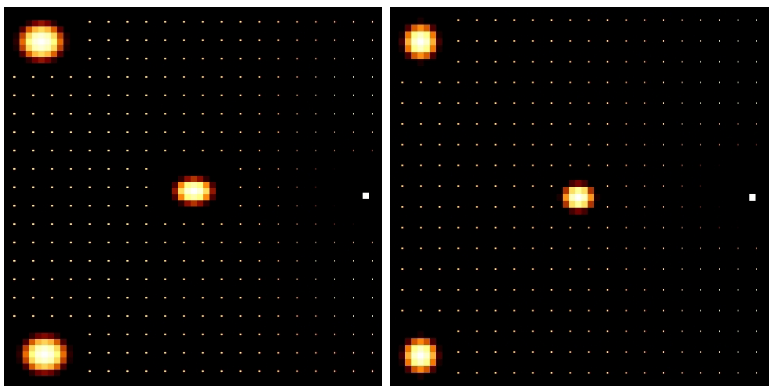

Figure 5. Comparison between a system using purely the TT-modes for correction and a system including the optimized scheme. The FOV is 4' x 4', the distance between the stars is 20", and the pixel scale of the stellar map is 0.″25 as is the LUCIFER pixel scale. To better emphasize the difference the color scale is logarithmic and some PSFs are enlarged. Left: PSF-map for the system correcting only the TT-modes, right: PSF-map for the optimized system. Note that the map shows the minimum achievable MSE at every position, i.e., the controller is optimized for this direction only.

3.2 Optimization over the full FOV

The application of the control scheme which will be used more often for a GLAO system is the optimization over the full FOV. This optimization will be under the aspect to gain a maximum homogeneity over the full FOV. This aspect however means that the difference between the wavefront MSEs in every two different directions is minimized. In formulas this reads:

$$\epsilon^2 \quad = \quad \int d\rho W(\rho) < (\phi_1(R\rho))^2 > + \sum_{i=2}^{N} \sum_{j=j_0}^{N_j} \left[-2P_{ij} < y_{1i}, x_j > + \sum_{k=k_0}^{N_k} P_{ij} P_{ik} < x_j, x_k > \right] - \tag{16}$$

$$\int d\rho W(\rho) < (\phi_2(R\rho))^2 > + \sum_{i=2}^{N} \sum_{j=j_0}^{N_j} \left[2P_{ij} < y_{2i}, x_j > - \sum_{k=k_0}^{N_k} P_{ij} P_{ik} < x_j, x_k > \right] = min$$

As the terms quadratic in P_{ij} cancel this MSE cannot be minimized by a specific choice of P_{ij}. So homogeneity is only improved by a correction which is optimized for every direction simultaneously. In Figure 7 the correction of the TT-MSE optimized over the full FOV is compared to the MSE of the non-optimized system. Again the FOV is 4' x 4', the resolution of the MSE map is 20".

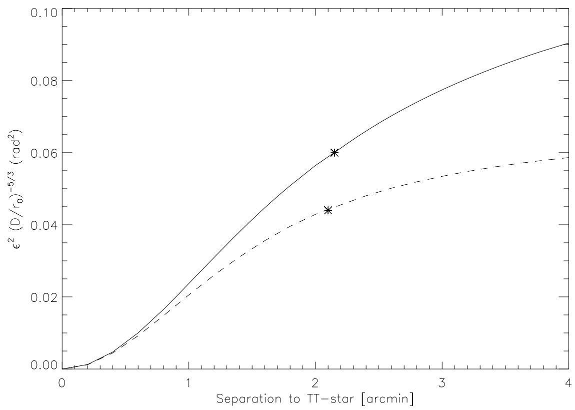

Figure 6. Plot of the MSE vs distance from TT-star. The MSE of the non-optimized system is plotted as solid line, the corresponding error of the optimized system is plotted as dashed line. The asterisks mark the corresponding average values.

Again the ratios between the maximum and average TT-MSEs of the two systems are compared. The ratio between the maximum MSE is $\epsilon^2_{max-Opt}/\epsilon^2_{max-NO} = 0.70$ and the ratio between the average MSE is $\epsilon^2_{av-Opt}/\epsilon^2_{av-NO} = 0.8$ still a significant difference.

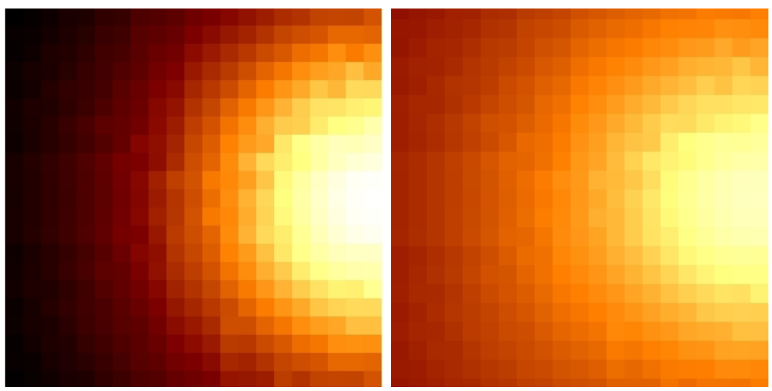

Figure 7. Comparison of the MSE between a system using purely the TT-modes for correction and a system including the optimized scheme. The FOV is 4' x 4', the resolution of the MSE map is 20". The color scale is the same for both maps. Left: TT-MSE correcting only the TT-modes, right: TT-MSE for the optimized system.

Figure 8 shows the PSF-maps corresponding to the MSE. The separation of the stars in the star field is 20", the FOV is 4' x 4', and the pixel scale of the star field is 0."25.

The values of the ratios between the maximum FWHMs of the two systems and the average FWHMs of the two systems number 0.84 and 0.89 respectively.
A further benefit from the averaged optimization over the full FOV is that the difference in the FWHM over the field is much reduced which improves the capability of comparing objects over the full FOV. The maximum variation of the homogeneity 'VH' of the FWHM will be defined as:

$$(FWHM_{max} - FWHM_{min})/FWHM_{av} \tag{17}$$

with $FWHM_{max}$ the maximum FWHM, $FWHM_{min}$ the minimum FWHM, and $FWHM_{av}$ the average FWHM. For the non-optimized system and the optimized system VH is 1.24 and 0.69 respectively. So the homogeneity is improved for the optimized system by almost a factor of 2.

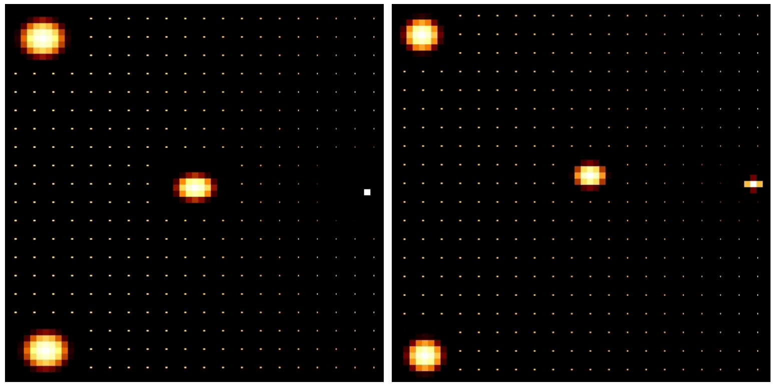

Figure 8. Comparison between a system using purely the TT-modes for correction and a system including the optimized scheme. The FOV is 4' x 4', the distance between the stars is 20", and the pixel scale of the stellar map is 0."25 as is the LUCIFER pixel scale. The color scale is chosen logarithmically to emphasize the difference. Also some of the PSFs are enlarged. Left: PSF-map for the non-optimized system, right: PSF-map of the optimized system.

Figure 9 shows the MSE with distance from the TT-star. The solid line marks the result for the non-optimized system, the dashed line the result for the optimized system. The average value is marked by the asterisks on each curve. The large improvement in homogeneity is obvious.

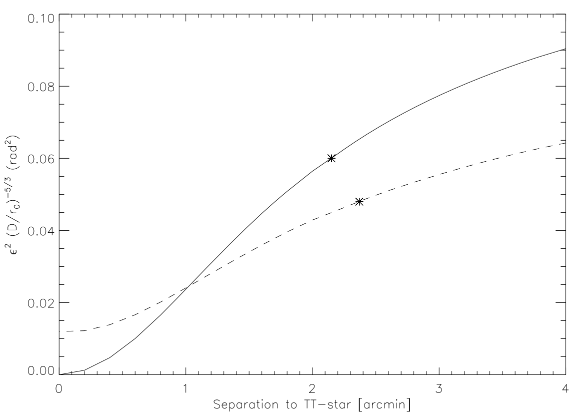

Figure 9. Plot of the MSE with distance from the TT-star. The MSE of the non-optimized system is plotted as solid line, the corresponding error of the optimized system is plotted as dashed line. The asterisks mark the corresponding average values.

4. CONCLUSIONS

I presented a scheme to improve the Tip-Tilt correction of the ARGOS system over the full field of view especially with regard to the homogeneity of the point spread function over the field of view. The scheme makes use of the measurements of high order modes of the three laser guide stars to add information to the measurements of the tip-tilt star. The effect of the inclusion of the laser measurements into the Tip-tilt-correction were presented for two cases: Optimizing the tip and tilt in a single direction anywhere in the field and optimization of the Tip-Tilt-signal over the full field of view. The calculation was performed for a 6 layered atmosphere with a seeing of 1".

In the first case the Tip-Tilt-correction was better at any field position except the position of the Tip-Tilt-star where the correction was equally good for both systems. On average the improvement of the mean square error over the field was 27% and maximum 36%.

In the case of the correction over the full FOV the performance around the position of the Tip-Tilt-star was reduced but improved in most of the other directions. On average the improvement of the tip tilt mean square error was 20% and at maximum 30%.
This had the additional benefit that the full width at half maximum of the point spread function over the full field of view was much more homogeneous in the case of the optimized controller. The homogeneity of the full width at half maximum at over the field as defined in the paper was improved by a factor of about 2.
The same concept can also be used to improve the homogeneity in the HO modes. As they are already averaged over three directions the gain will be much smaller, i.e., will hardly be noticed in a GLAO system. However, for different applications, i.e. MCAO, the scheme presented here might well be applicable for the HO-modes also. This will be investigated in the future.

ACKNOWLEDGMENTS

The author wants to thank the ARGOS team especially W.Gässler for helpful discussions. ARGOS is partly funded through the European Framework Program 7 within OPTICON (grant agreement no 226604).

REFERENCES

[1] Rabien, S. et al., "ARGOS the laser guide star system for LBT", 7736-13 (this conference)

[2] Mandel, H. et al., "LUCIFER status report: summer 2008", Proc.SPIE, 7014, 124 (2008)

[3] Tokovinin, A. A., "From Differential Image Motion to Seeing", PASP, 114, 1156 (2002)

[4] Tokovinin, A. A. et al., "Statistics of turbulence profile at Cerro Tololo", MNRAS, 340, 52 (2003)

[5] Wilson, R. W., "SLODAR: measuring optical turbulence altitude with a Shack-Hartmann wavefront sensor", MNRAS, 337, 103 (2002)

[6] Poyneer, L. et al., "Experimental verification of the frozen flow atmospheric turbulence assumption with use of astronomical adaptive optics telemetry", JOSAA, 26, 833 (2009)

[7] Whiteley, M. R., "Optimal modal wave-front compensation for anisoplanatism in adaptive optics", JOSAA, 15, 2097 (1998)

[8] Peter, D., "Point-spread function reconstruction for the ground layer adaptive optics system ARGOS", 7736-177 (this conference)